Deciphering Mechanochemical Influences of Emergent Actomyosin Crosstalk using QCM-D

Emily M. Kerivan[1], Victoria N. Amari[1], William B. Weeks[1], Leigh H. Hardin[1], Lyle Tobin[1], Omayma Y. Al Azzam[2], and Dana N. Reinemann*[1,2]

[1]Department of Biomedical Engineering, [2]Department of Chemical Engineering, University of Mississippi, University, MS, USA 38677

*Corresponding Author: dnreinem@olemiss.edu

Justification

Cytoskeletal ensembles exhibit mechanics that are not necessarily the sum of the components' single molecule properties, and this emergent behavior is not well understood. Cytoskeletal filaments may also act as force sensors that influence constituent motor protein behavior. To understand the elusive design principles of such emergent mechanics, we innovated an approach using QCM-D to measure how actomyosin bundles sense and respond mechanically to environmental variables. We demonstrate for the first time that QCM-D can detect changes in actomyosin viscoelasticity due to molecular-level alterations, thus providing evidence for actin's role as a mechanical force-feedback sensor and a new approach for deciphering the fundamentals of emergent cytoskeletal ensemble crosstalk.

Abstract

Cytoskeletal protein ensembles exhibit emergent mechanics where behavior exhibited in teams is not necessarily the sum of the components' single molecule properties. In addition, filaments may act as force sensors that distribute feedback and influence motor protein behavior. To understand the design principles of such emergent mechanics, we developed an approach utilizing QCM-D to measure how actomyosin bundles respond mechanically to environmental variables that alter constituent myosin II motor behavior. We demonstrate that QCM-D can detect changes in actomyosin viscoelasticity due to molecular-level alterations, such as motor concentration and nucleotide state, thus providing evidence for actin's role as a mechanical force-feedback sensor and a new approach for deciphering the fundamental mechanisms of emergent cytoskeletal ensemble crosstalk.

The cytoskeleton consists of elements such as filaments, crosslinkers, and motor proteins that have vastly different mechanical, motile, and force generating capabilities yet work concertedly to perform large-scale tasks, such as cell division and translocation.[1,2] In many cases, when the cytoskeleton is studied *in vitro*, investigators are considering one family of the cytoskeleton at a time (e.g. actin and myosin or microtubules and kinesin) and are often working close to the single molecule level.[2,3] While single molecule studies have revealed invaluable information about motor protein properties such as processivity, stepping, and force generation capability, studies are increasingly finding that new behaviors emerge when motors, proteins, and filaments begin working together in groups that are not the sum of the constituent single molecule properties.[1,2,4] The design principles behind these emergent cytoskeletal mechanics are not yet understood but will be necessary for understanding the basic rules of life, as well as applications like building synthetic cells, deciphering mechanisms of cytoskeletal-based diseases, and engineering smart materials.[4–8]

Actomyosin emergent mechanics are especially interesting as myosin II behavior is strikingly different between the single molecule level and when in ensembles. As a single molecule, myosin II is not processive, or it does not take multiple steps along an actin filament (AF) before diffusing away, and it has a relatively low force generation capacity of a few piconewtons and a number of different reported step sizes, such as 5 nm, 11 nm, and 30 nm.[2,9–15] However, when myosin II works in groups, processivity and force generation increase, though not necessarily in a linear fashion with the number of motors present.[2,4,5,7,8,16–24] Various approaches have been taken to investigate myosin II ensemble behavior, such as adapting the three-bead optical trapping assay to have

multiple motors attached to a bead, adapting the gliding filament assay to measuring unloaded velocity and loaded force generation, or measuring force generation capacity of a thick filament of myosins against a suspended AF.[7,8,20,21] While these approaches yielded valuable information about behavior deviation between single myosins and those in ensembles, limitations in assay design exist, such as having the myosins attached to a rigid bead or coverslip surface and having their relative orientation fixed due to their attachment. In order to probe how motor self-optimization and AF compliancy affect myosin II ensemble dynamics, Al Azzam *et al.* designed an optical trapping assay to investigate teams of myosin II motors within AF bundles.[4,5] They found that ensemble myosin II motility and force generation depend on its local environment.[4] The relative concentration and thus attachment of myosin II motors to the AF bundles change the local stiffness of the AF, dictating force generation capability and step sizes of the myosins.[4] The effect of myosin II motor activity on AF stiffness has also been demonstrated at the bulk AF mesh level, especially when in concert with other static AF crosslinkers.[25–28] Al Azzam's results, in conjunction with previous rheological studies of bulk AF systems, suggest that a force-feedback mechanism may exist that is mediated by the AF serving as a mechanical force sensor. Other studies have hypothesized that AFs act as a local and systemic force sensor as well, pointing to emergent changes within the actomyosin cytoskeleton that take place based off of function-specific needs.[29,30] However, how these physical signals translate to the molecular actuators and how emergent force-feedback loops are controlled within motor ensembles remain a gap in knowledge.[30,31] Understanding the design principles of motor-filament system compliancy influences

within cytoskeletal ensembles would aid in filling this gap, but accessible methods to probe these properties are lacking.

A quartz crystal microbalance with dissipation monitoring (QCM-D) is an instrument that uses a piezoelectric sensor to detect ng-level changes in mass, as well as changes in viscoelasticity in systems attached to the sensor surface.[32–34] While QCM-D has traditionally been used to study properties of coatings and polymers, it has started to gain traction in the biophysics field to study changes in mechanical properties of biological materials.[32,35] Applications for QCM-D in studying the cytoskeleton have been reviewed by Kerivan *et al.*[32] Most cytoskeletal applications involve studying how cells deform in response to a stimulus or drug. There have been *in vitro* cytoskeletal studies that focus more on binding mechanisms of motors and filaments, as well as gaining a better understanding of how classic *in vitro* motility assays assemble and behave on a non-physiological surface, like a coverslip.[36–41] This is important to understand because methods for constructing model *in vitro* experiments will influence subsequent measurements and thus constrain how well we can correlate *in vitro* experiments to *in vivo* phenomena. However, to our knowledge, no one has used QCM-D to investigate the assembly of hierarchically structured cytoskeletal filament and motor ensembles, as well as monitor changes in system viscoelasticity in real time. In order to better understand how AFs may be acting as a force sensor that drives the force-feedback mechanism between the myosin motors and AFs, we developed an approach using QCM-D to investigate the emergent mechanics of actomyosin ensembles.

A QSense Analyzer QCM-D system from Biolin Scientific and their standard gold sensors were used to gather frequency and dissipation measurements for actomyosin

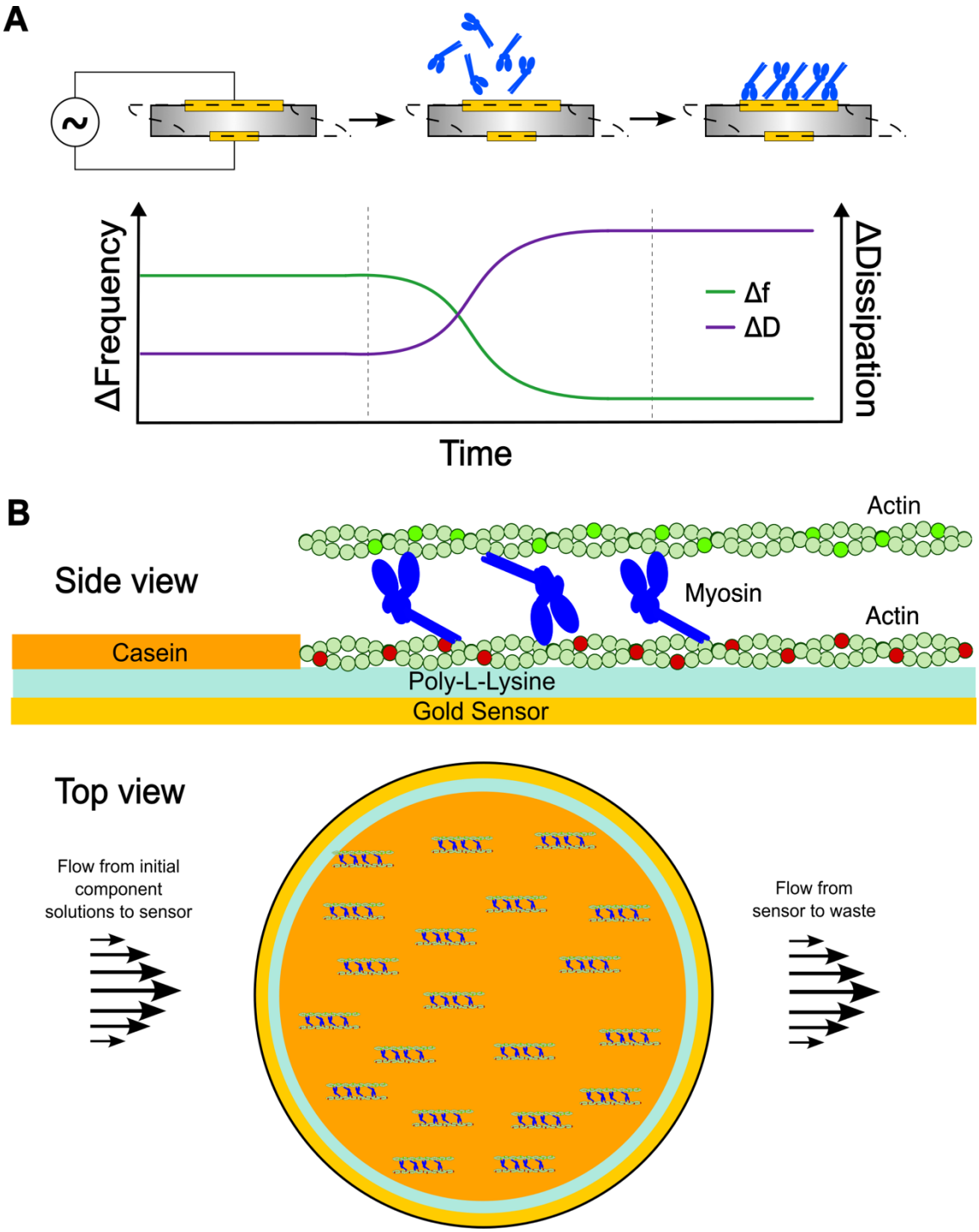

Figure 1 | Principles of QCM-D operation and assay schematic. (A) As mass is added to the piezoelectric sensor, frequency decreases. As viscoelasticity of the sensor "coating" changes from rigid to soft, dissipation increases. Adapted from Kerivan *et al.* (2023) *Cytoskeleton*. Reproduced with permission from Wiley under license number 5633140041004. (B) Side and top view of how the actomyosin bundles were assembled onto the gold sensors. After an initial wash with general actin buffer, the following components were introduced via the QSense pump: poly-l-lysine, actin, casein, myosin, actin, and a final buffer wash. Schematics are not drawn to scale.

bundle formation (Figure 1). With QCM-D, a decrease in frequency corresponds with the piezoelectric sensor being damped due to mass addition (Figure 1A).[32,33] Dissipation monitoring of the QSense system allows for measuring relative viscoelastic changes in samples, denoted by an increase in dissipation when a sample becomes “softer”.[32,33] To mimic conditions on the gold sensor similarly to what was measured in the optical trapping experiments from Al Azzam *et al*., the actomyosin bundles were built from the bottom up onto the sensor surface. First, if not using a new sensor, the gold sensor must be cleaned thoroughly using either a sodium dodecyl sulfate solution and exposure to an ozone chamber, or piranha solution. Sensor cleanliness and age can greatly affect frequency and dissipation measurements if debris is left on the sensor from previous experiments, so care must be taken to maintain high quality sensors. Solutions of poly-l-lysine (PLL 30 μL of 0.1% PLL solution in 30 mL of DI water), actin (200 μL in 1 mL), casein (1 mg in 15 mL), full length skeletal myosin II (0.6 μM), and general actin buffer (GAB, contents) were prepared before measurements and kept on ice until ready to use. As in the previous optical trapping experiments, PLL is used to coat the sensor surface to facilitate AF binding, and casein is used as a blocking agent to prevent non-specific binding of subsequent proteins to the sensor surface.[4,5] There must be enough volume of each solution made in order to cover the sensor surface and reach a plateau in the frequency and dissipation measurements. With the peristaltic pump set to 0.1 mL/min and anywhere from 10-30 minutes required to reach a plateau in measurement, this required at least 1-3 mL necessary for each component of the assay. This can be somewhat difficult when using expensive protein reagents, such as actin and myosin, to ensure that you have enough protein present for the experiment.

After the solutions were prepared, they were added into the QSense system and onto the gold sensor surface using the built-in microfluidic system and peristaltic pump. To achieve a baseline measurement, general actin buffer (GAB) was introduced first, and the frequency and dissipation signals were allowed to stabilize. Next, the dilute PLL solution was added to coat the sensor surface. We also tried pre-coating the gold sensors with PLL as would be done with coverslips in an optical trapping flow cell assay; however, we found subsequent component addition steps and the frequency and dissipation measurements to be more consistent when adding in the PLL with the pump and letting it settle. Subsequently, the solutions of actin, casein, myosin II, actin, and GAB were added via the pump onto the sensor and allowed to settle over approximately 15-minute periods. We note that we also tried implementing wash steps between the additions of the different reagents (see Figure S1). However, this significantly increased the time of an already lengthy experiment with minimal benefit to obtaining clean frequency and dissipation shift measurements.

A representative trace of frequency and dissipation shifts for actomyosin bundle formation is shown in Figure 2. Additional example traces can be found in Figure S1. Several overtone measurements are recorded by the QSense Analyzer with differing balances of signal and sensitivity; overtone 7 exhibits a consistent balance and is used for subsequent analysis. The time to plateau for each component addition varies depending on the concentration of the reagents but is usually around 15 minutes. Again, frequency decrease represents mass addition, and dissipation increase is a change in system viscoelasticity from rigid to more compliant. Changes in frequency and dissipation are minimal for GAB and PLL, as would be expected. The first actin addition settles out

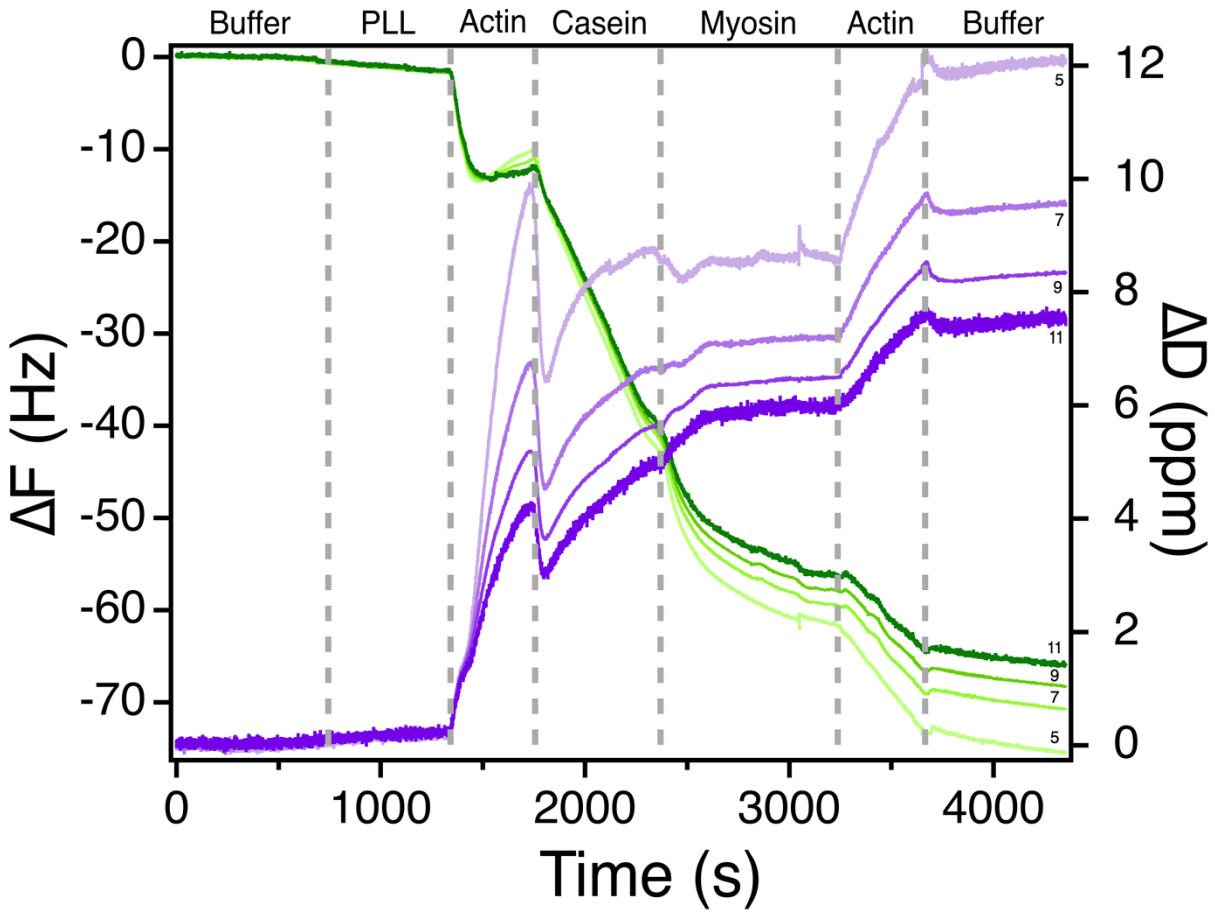

Figure 2 | Actomyosin bundle assembly dynamics using QCM-D. Change in frequency (green) and dissipation (purple) at multiple overtones for each component of the *in vitro* actomyosin bundle assay. These results verify that QCM-D experiments are able to sense molecular-level binding, dynamics, and changes in viscoelasticity of cytoskeletal ensemble systems in real time.

relatively quickly in frequency, and a large positive shift in dissipation is apparent, which makes sense as a compliant protein filament is introduced onto the piezoelectric sensor. Casein, the surface blocker, is clearly adding mass, yet the dissipation increase is not as high as for actin since casein is able to evenly and tightly coat the surface. Subsequent additions of myosin and actin show significant changes in frequency and dissipation, especially once actin is added, binds myosin, and makes the final bundle connection onto the sensor surface. A final buffer wash is introduced to ensure that the actomyosin bundles have indeed formed, do not wash away, and serves as a control to demonstrate

that introducing more fluid with no proteins to bind the existing bundle does not change the conditions of bundle bound to the sensor surface. These results demonstrate that forming structured, hierarchical cytoskeletal assemblies on a QCM-D sensor is not only feasible, but clear changes in dissipation and thus system viscoelasticity can be observed.

We next wanted to evaluate what types of environmental parameter changes could be measured within actomyosin bundles using QCM-D. As stated earlier, myosin II concentration and activity have been shown to alter systemic force generation in an emergent manner.[4] As more heads are recruited and bound to AFs, the local environment is less compliant, leading to a sensory-force feedback mechanism of motor activity within the AF bundle.[4] Thus, we altered myosin concentration to verify that such changes would be measurable with QCM-D. We were also interested in knowing whether changes in small molecules, such as nucleotides, would also be detectable with QCM-D as myosin exhibits a different conformational state and tighter AF binding when ADP is bound than with ATP, thus further altering local system stiffness. Figure 3 demonstrates that lowering myosin concentration from 3A to 3B can indeed be detected as lower shifts in frequency and dissipation while the relative changes in frequency and dissipation shifts for both the first and second actin additions are relatively similar. Strikingly, the buffer washes with different nucleotides also yielded unique signatures in frequency and dissipation shifts. In Figure 3, both “buffer” washes are with general actin buffer (GAB) that is supplemented with ATP. Further, all additions of PLL, actin, casein, and myosin are all diluted in GAB. In Figure 3A, frequency shifts very little with buffer addition, which would be expected since we are not adding any substantial mass. However, dissipation shifts significantly

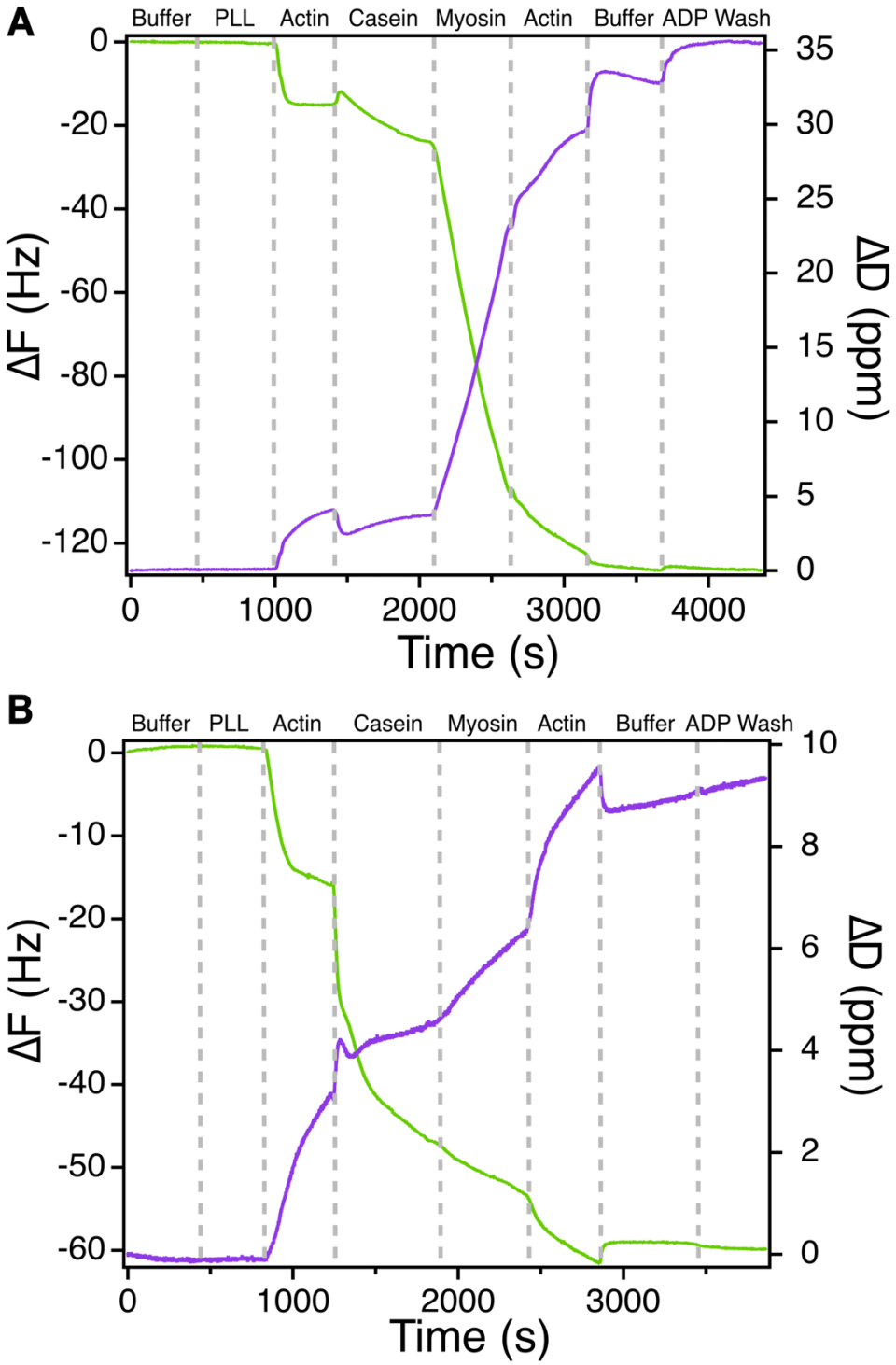

Figure 3 | Influences of motor concentration and nucleotide state. (A) Actomyosin bundle assembly with a higher concentration of myosin II motors and concluding with a GAB-ADP supplement wash. (B) The lower concentration of myosin II in bundle assembly is detected, as well as motor activation in the first GAB wash and nucleotide change to ADP in the second wash. In both (A) and (B), motor activation commensurate with the relative motor concentration is observed, as well as increased bundle formation due to the addition of ADP.

initially and then levels out. This positive shift indicates that the system is becoming less rigid. This wash would be removing any remaining unbound actin from the previous step as well as introducing fresh ATP and thus an increase in motor activity in the actomyosin bundles. This is also seen in Figure 3B for the buffer wash. The frequency does increase slightly, indicating a removal of mass, which is feasible as there is likely some level of unbound actin left, but it certainly does not completely wash out the bundle structure that was form as it levels out quickly. However, dissipation continues to increase, not at the rate as seen in Figure 3A, but there are fewer myosin motors in each relative bundle at this point in Figure 3B. Yet, there is still an increase in system softness, suggesting that increasing motor activity alters the viscoelasticity of the local actomyosin system. This correlates with results from Koenderink *et al.* where myosin activity in AF meshes leads to increased viscous dissipation in comparison to a passive actin solution.[28] This is further seen with the ADP wash where the same GAB buffer is used except ATP is substituted with the same concentration of ADP. Additional example traces can be found in Figure S2. In both Figures 3A and 3B, we do not see much change in frequency at all, which would be expected since, again, we are not adding any components with substantial mass. However, in each case, there is a striking increase in dissipation, much more so in Figure 3A likely due to more myosin motors present in the bundles thus enhancing the effect. ADP increases the binding affinity of myosin II for actin but also renders myosin inactive; so, one might initially expect for dissipation to decrease, or the system getting relatively more rigid with the addition of ADP. This would likely be the case with large-scale AF mesh measurements as measured previously.[26,28] However, by increasing the binding affinity of myosin for AFs in dilute bundle conditions, we are also increasing the

probability of forming more actin-myosin-actin connections. Thus, collectively across the sensor surface, more actomyosin bundles connections yield an overall more viscoelastic "coating" that is detected.

The actomyosin bundle QCM-D results here are complementary to our previous force generation changes measured by optical tweezers[5]. Myosin II group dynamics, such as stepping and force generation, are significantly different depending on the local environment in which they were working. In addition, it is known that myosin II as a single molecule is non-processive, yet when in groups, they processively work together. But how do the motors know whether to be in a low or high duty ratio mode? We hypothesize that there are two levels of sensory-force feedback: motor-motor communication and more systemically through the AF.[4] Contributions could be due to myosins existing in a semi-diffusive state with the ability to entropically expand (directional ensemble movement due to diffusion) with some level of force contribution.[4,42] It may also be due to the number of motors that are attached, as saturation of binding sites would require metachronal wave-like systematic communication in order for the myosins to be able to take forward steps without wasting energy.[43] In addition, the number of attached motors will change the mechanical properties of the AF (e.g. more motors attached increases AF stiffness) but may also influence pre-stress on the AF.[28,44,45] Thus, emergent AF compliancy may communicate to distal motors which duty ratio mode is needed for the function at hand.[30,31] Through the QCM-D results presented, we observe such changes in mechanical compliancy of *in vitro* actomyosin systems due to changes in motor activity and concentration, further backing the hypothesis that actin filaments can serve as a force sensor and mediator of feedback to its bound motors and local environment.[4,29–31,46]

The ability of QCM-D to detect molecular level changes in mass and viscoelasticity in cytoskeletal ensemble systems will open doors for a variety of applications and experiments that complement existing techniques, such as total internal reflection fluorescence microscopy, atomic force microscopy, and optical trapping. Further assay customizations could be explored, such as using different sensor cleaning protocols, coatings, and surface modifications. For instance, one could use silicon dioxide sensors to more closely mimic coverslips used for microscopy experiments or buy protein-coated sensors, such as biotin. Experiments could also be expanded to other cytoskeletal systems and motor proteins as the addition of environmental influences, such as crowding agents, ionic strength, and crosslinkers have been suggested to influence motor behavior.[30,31,47–49] For example, the effect of flexible crosslinkers like filamin A alone or myosin II motors alone in AF meshes have marginal influences on system stiffening, yet when combined, have significant emergent effects on stiffness and activity.[28] Increasing the complexity of these *in vitro* ensembles will approach more physiologically relevant conditions to then compare how their systemic viscoelasticity changes correlate with motility or force generation changes in TIRF or optical trapping experiments, respectively. However, there are pitfalls that remain in probing cytoskeletal assemblies using QCM-D. For instance, the QSense Analyzer has included software that will provide estimates of Young's modulus, coating thickness, and mass added to the sensor. One of the major assumptions of the Sauerbrey equation used for detecting mass and then ultimately obtaining estimates for modulus is that the sensor has a complete, homogenous, and rigid coating of even thickness. That is certainly not the case with this particular application as we are using multiple proteins of different sizes and compliances, but what

likely has more influence is the non-uniformity of the “coating” thickness, as schematically shown in Figure 1B. Perhaps this would be less of an issue when exploring large-scale AF meshes, but when attempting to characterize small motor ensemble properties, the sensor is not evenly coated. Thus, correction factors or different models would need to be developed and adapted with the software in order to use them for quantitative analysis. However, with strict controls and notes of when design parameters are changed, the real-time measurement of frequency and dissipation changes within cytoskeletal systems can be compared amongst each other to determine how potential mechanical influencers, such as different protein types, environmental buffer conditions, or nucleotide state, alter the cytoskeletal ensemble’s mechanics. Other potential downsides to these experiments are the high concentrations of protein required and the time required per experiment with our longest runs being almost two hours of data, but that does not include the fresh protein solution preparations and sensor and QCM module cleaning required before and after use. One should also consider how QCM-D data would supplement their specific mechanistic inquiry. Until improved models are developed for quantitatively interpreting QCM-D frequency and dissipation change measurements for cytoskeletal ensembles, it would be beneficial to couple the qualitative information regarding changes in assay conditions and system viscoelasticity with quantitative force measurement techniques, like AFM or optical tweezers, or in conjunction with fluorescence microscopy.[32] For example, Yang *et al.* characterized cell-level mechanical behavior of epithelial cells in response to epidermal growth factor (EGF) using a combination of fluorescence imaging to capture the response of actin filaments, AFM to probe the cell’s mechanical response, and QCM-D to correlate energy with the measured AFM response to EGF stimulation.[50]

Their approach demonstrates the advantage of using complementary techniques to formulate a more complete biophysical profile of their system of interest and should be applied more readily to *in vitro* studies.

In conclusion, we demonstrate that QCM-D is a useful tool that complements existing experimental approaches in systematically characterizing the interconnection of force, mechanics, and machinery within cytoskeletal ensembles and can be used to decipher which mechanical cues lead to certain ensemble behaviors.[51] QCM-D will especially be helpful in constructing more thorough biophysical profiles of cytoskeletal ensembles through identifying the molecular parameters that dictate emergent mechanical behavior and revealing clues towards the design principles of regulatory feedback behavior at the molecular level that then propagates up in scale to influence long-distance cellular tasks.

Acknowledgements

This work is supported by the American Heart Association #848586, NIH R35 GM147050, NSF REU Site: Ole Miss Nanoengineering Summer REU Program NSF ENG/EEC #2148764, and the Mississippi Space Grant Consortium under grant number NNX15AH78H. QCM-D instrumentation, data, and analysis are supported by NSF MRI grant number 2018004. The shared QCM-D facility at the University of Mississippi is open to outside collaboration. If interested, contact qcmd@olemiss.edu.

Author Contributions

EMK and DNR conceptualized the work. EMK, VNA, WBW, LHH, LT, and OYA developed and optimized the protocols. EMK, VNA, WBW, and LHH gathered and analyzed the data. EMK, VNA, and DNR wrote and edited the manuscript.

Supplemental Information

Detailed methods and additional QCM-D traces can be found in the supplemental information.

References

1 S. Dumont and M. Prakash, *Mol. Biol. Cell*, 2014, **25**, 3461–3465.

2 O. Al Azzam, C. L. Trussell and D. N. Reinemann, *Cytoskeleton*, 2021, **78**, 111–125.

3 M. W. Elting and J. A. Spudich, *Dev. Cell*, 2012, **23**, 1084–1091.

4 O. Y. Al Azzam, J. C. Watts, J. E. Reynolds, J. E. Davis and D. N. Reinemann, *Cell. Mol. Bioeng.*, 2022, **15**, 451–465.

5 O. Al Azzam, J. C. Watts, J. E. Reynolds, J. E. Davis and D. N. Reinemann, *J. Vis. Exp.*, 2022, 1–20.

6 T. J. Stewart, V. Murthy, S. P. Dugan and J. E. Baker, *J. Biol. Chem.*, 2021, **297**, 101178.

7 M. Kaya, Y. Tani, T. Washio, T. Hisada and H. Higuchi, *Nat. Commun.*, 2017, **8**, 1–13.

8 S. Walcott, D. M. Warshaw and E. P. Debold, *Biophys. J.*, 2012, **103**, 501–510.

9 J. T. Finer, R. M. Simmons and J. a Spudich, *Nature*, 1994, **368**, 113–119.

10 C. B. O'Connell, M. J. Tyska and M. S. Mooseker, *Biochim. Biophys. Acta - Mol. Cell Res.*, 2007, **1773**, 615–630.

11 J. Howard, *Mechanics of Motor Proteins and the Cytosksleton*, 2001.

12 C. Ruegg, C. Veigel, J. E. Molloy, S. Schmitz, J. C. Sparrow and R. H. A. Fink, *Physiology*, 2002, **17**, 213–218.

13 J. E. Molloy, J. E. Burns, J. C. Sparrow, R. T. Tregear, J. Kendrick-Jones and D. C. White, *Biophys. J.*, 1995, **68**, 298S-303S; 303S-305S.

14 M. J. Tyska, D. E. Dupuis, W. H. Guilford, J. B. Patlak, G. S. Waller, K. M. Trybus,

D. M. Warshaw and S. Lowey, *Proc. Natl. Acad. Sci. U. S. A.*, 1999, **96**, 4402–4407.

15 K. Kitamura, M. Tokunaga, A. H. Iwane and T. Yanagida, *Biophys. J.*, 1999, **76**, A36--A36.

16 J. A. Wagoner and K. A. Dill, *Proc. Natl. Acad. Sci. U. S. A.*, , DOI:10.1073/pnas.2101871118.

17 J. Sung, S. Nag, K. I. Mortensen, C. L. Vestergaard, S. Sutton, K. Ruppel, H. Flyvbjerg and J. A. Spudich, *Nat. Commun.*, 2015, **6**, 1–9.

18 C. Liu, M. Kawana, D. Song, K. M. Ruppel and J. A. Spudich, *Nat. Struct. Mol. Biol.*, 2018, **25**, 505–514.

19 M. J. Greenberg and J. R. Moore, *Cytoskeleton*, 2010, **67**, 273–285.

20 E. P. Debold, S. Walcott, M. Woodward and M. A. Turner, *Biophys. J.*, 2013, **105**, 2374–2384.

21 M. Kaya and H. Higuchi, *Science (80-.).*, 2010, **329**, 686–689.

22 L. Hilbert, S. Cumarasamy, N. B. Zitouni, M. C. Mackey and A. M. Lauzon, *Biophys. J.*, 2013, **105**, 1466–1474.

23 M. R. Stachowiak, P. M. McCall, T. Thoresen, H. E. Balcioglu, L. Kasiewicz, M. L. Gardel and B. O'Shaughnessy, *Biophys. J.*, 2012, **103**, 1265–1274.

24 T. J. Stewart, D. R. Jackson, R. D. Smith, S. F. Shannon, C. R. Cremo and J. E. Baker, *Cell. Mol. Bioeng.*, 2013, **6**, 26–37.

25 T. B. Liverpool, A. C. Maggs and A. Ajdari, *Phys. Rev. Lett.*, 2001, **86**, 4171–4174.

26 D. Humphrey, C. Duggan, D. Saha, D. Smith and J. Käs, *Nature*, 2002, **416**, 413–416.

27 F. Ziebert and I. S. Aranson, *Phys. Rev. E - Stat. Nonlinear, Soft Matter Phys.*, 2008, **77**, 1–5.

28 G. H. Koenderink, Z. Dogic, F. Nakamura, P. M. Bendix, F. C. MacKintosh, J. H. Hartwig, T. P. Stossel and D. A. Weitz, *Proc. Natl. Acad. Sci. U. S. A.*, 2009, **106**, 15192–15197.

29 T. Luo, K. Mohan, P. A. Iglesias and D. N. Robinson, *Nat. Mater.*, 2013, **12**, 1064–1071.

30 X. Sun and G. M. Alushin, *FEBS J.*, 2022, **290**, 2576–2589.

31 A. Jégou and G. Romet-Lemonne, *Curr. Opin. Cell Biol.*, 2021, **68**, 72–80.

32 E. M. Kerivan, L. Tobin, M. Basil and D. N. Reinemann, *Cytoskeleton*, 2023, **80**, 100–111.

33 M. C. Dixon, *J. Biomol. Tech.*, 2008, **19**, 151–158.

34 Biolin Scientific, 2017, 1–2.

35 B. Scientific, Characterization of biomolecular interactions: Analysis of adsorption, binding, and enzymatic action with QSense QCM-D.

36 N. Albet-Torres, A. Gunnarsson, M. Persson, M. Balaz, F. Höök and A. Månsson, *Soft Matter*, 2010, **6**, 3211–3219.

37 N. Albet-Torres, J. O'Mahony, C. Charlton, M. Balaz, P. Lisboa, T. Aastrup, A. Månsson and I. A. Nicholls, *Langmuir*, 2007, **23**, 11147–11156.

38 M. Persson, N. Albet-Torres, L. Ionov, M. Sundberg, F. Höök, S. Diez, A. Månsson and M. Balaz, *Langmuir*, 2010, **26**, 9927–9936.

39 H. Suda, N. Sasaki, Y. C. Sasaki and K. Goto, *Eur. Biophys. J.*, 2004, **33**, 469–476.

40 K. L. Hanson, V. Viidyanathan and D. V. Nicolau, *BioMEMS Nanotechnol. II*, 2005,

6036, 603602.

41 H. Van Zalinge, J. Aveyard, J. Hajne, M. Persson, A. Mansson and D. V. Nicolau, *Langmuir*, 2012, **28**, 15033–15037.

42 O. Kučera, V. Siahaan, D. Janda, S. H. Dijkstra, E. Pilátová, E. Zatecka, S. Diez, M. Braun and Z. Lansky, *Nat. Commun.*, 2021, **12**, 1–12.

43 M. Mitsuka, T. Yamada and H. Shimizu, *J. Biochem.*, 1979, **85**, 559–565.

44 S. Lin, X. Han, G. C. P. Tsui, D. Hui and L. Gu, *Compos. Part B Eng.*, 2017, **116**, 377–381.

45 Y. E. Goldman and A. F. Huxley, *Biophys. J.*, 1994, **67**, 2131–2133.

46 T. L. Chen, Z. Dai, P. Mo, X. Li, Z. Ma, S. Song, X. Chen, M. Luo, K. Liang, S. Gao, Y. Zhang, L. Deng, Y. Xiong and A. Newman, *Journals Gerontol. - Ser. A Biol. Sci. Med. Sci.*, 2020, **75**, 1788–1795.

47 S. Nagy, B. L. Ricca, M. F. Norstrom, D. S. Courson, C. M. Brawley, P. A. Smithback and R. S. Rock, *Proc. Natl. Acad. Sci. U. S. A.*, 2008, **105**, 9616–9620.

48 T. Iwase, Y. Sasaki and K. Hatori, *Biochim. Biophys. Acta - Gen. Subj.*, 2017, **1861**, 2717–2725.

49 G. Lee, G. Leech, P. Lwin, J. Michel, C. Currie, M. J. Rust, J. L. Ross, R. J. McGorty, M. Das and R. M. Robertson-Anderson, *Soft Matter*, 2021, **17**, 10765–10776.

50 R. Yang, J. Y. Chen, N. Xi, K. W. C. Lai, C. Qu, C. K. M. Fung, L. S. Penn and J. Xi, *Exp. Cell Res.*, 2012, **318**, 521–526.

51 M. Lang, *Bridg.*, 2007, **37**, 11–16.